

## MD STUDIES ON CONFORMATIONAL BEHAVIOR OF A DNA PHOTOLYASE ENZYME

*E. Dushanov*<sup>a,b</sup>, *Kh. Kholmurodov*<sup>a,c</sup>, *K. Yasuoka*<sup>d</sup>, *E. Krasavin*<sup>a,c</sup>

<sup>a</sup> Joint Institute for Nuclear Research, Dubna

<sup>b</sup> Institute of Nuclear Physics, Ulugbek, Tashkent

<sup>c</sup> Dubna International University, Dubna, Russia

<sup>d</sup> Department of Mechanical Engineering, Keio University, Yokohama, Japan

In this work, molecular dynamics (MD) simulations were performed on a DNA photolyase protein with two cofactors, FAD (flavin adenine dinucleotide) and MTHF (methenyltetrahydrofolate), inside the enzyme pocket. A DNA photolyase is a highly efficient light-driven enzyme that repairs the UV-induced cyclobutane–pyrimidine dimer in damaged DNA. We were aimed to compare the conformational changes of the FAD cofactor and other constituent fragments of the molecular system under consideration. The conformational behavior of the FAD molecule is very important for understanding the functional and structural properties of the DNA repair protein photolyase. The photoactive FAD is an essential cofactor both for specific binding to damaged DNA and for catalysis. The second chromophore (MTHF or 8-HDF) is not necessary for catalysis and has no effect on specific enzyme — substrate binding. The obtained results were discussed to gain insight into the light-driven mechanism of DNA repair by a DNA photolyase enzyme — based on the enzyme structure, the FAD mobility, and conformation shape.

Выполнено молекулярно-динамическое моделирование ДНК-фотолиазы с целью изучить конформационное поведение фотоактивного кофактора флавин-аденин-динуклеотида (FAD) внутри полости фермента. ДНК-фотолиаза — высокоэффективный, активируемый светом фермент, восстанавливающий индуцированный ультрафиолетовым излучением циклобутан-пиримидиновый димер в поврежденной ДНК. Изучены конформационные и динамические изменения FAD во всей структуре белка ДНК-фотолиазы (включающей молекулы FADH, MTHF и ДНК) в водном растворе. Проведено сравнение конформационных изменений кофактора FAD и других фрагментов рассматриваемой молекулярной системы. На основе данных о структуре фермента, подвижности FAD и конформации системы полученные результаты обсуждены с точки зрения понимания активируемого светом механизма репарации ДНК ферментом ДНК-фотолиазой.

PACS: 83.10.Rs; 31.15.xv; 87.10.Tf; 87.15.ap; 47.11.Mn

### INTRODUCTION

The DNA photolyase enzyme repairs UV-induced DNA damage which is regarded to be one of the most common lesions of living organisms from the beginning of life formation on the Earth. On the early Earth with no good atmospheric shield, the UV (ultraviolet) radiation was allowed to penetrate deep into the Earth. Astrobiological knowledge indicates that the Earth surface in the early stages was not yet covered well with the stable atmosphere and it was

being much suffered from the negative UV effects [1]. Thus, from the early periods of time on the Earth, living organisms have developed against the DNA irradiation a number of self-defence and self-repair mechanisms inside the cell.

Under UV photon absorption, in living organisms a photoreaction of DNA pyrimidine bases, in particular, thymine dimers ( $T \leftrightarrow T$ , cyclobutane–pyrimidine dimers (CPDs)) could be formed. The  $T \leftrightarrow T$  dimer formation (Fig. 1), followed by a UV photon absorption with an excitation of a thymine monomer and a subsequent reaction to an adjacent thymine molecule, can brought to a number of harmful effects, such as growth delay, mutagenesis or cell death [2–6]. The DNA photolyase enzyme repairs damaged DNA, by splitting the ring of the predominant photoproduct — the *cis,syn*-CPD — back into the corresponding pyrimidine monomers [2–8].

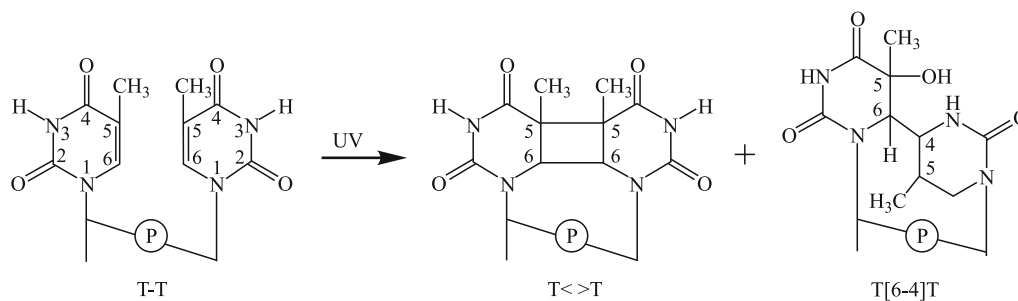


Fig. 1. The two major DNA lesions induced by UV radiation are cyclobutane–pyrimidine dimers (CPDs) and pyrimidine–pyrimidone (6-4) photoproducts. The figure shows the UV-induced DNA photoproducts that were formed between adjacent thymines. From [2–8]

Photolyases are monomeric proteins of 450–550 amino acids and two noncovalently bound chromophore cofactors (Fig. 2). One of the cofactors is always FAD (flavin adenine dinucleotide (Fig. 3, left)), and the second is either MTHF (methenyltetrahydrofolate (Fig. 3, right)) or 8-HDF (8-hydroxy-7,8-didemethyl-5-deazari-boavin). The latter, MTHF

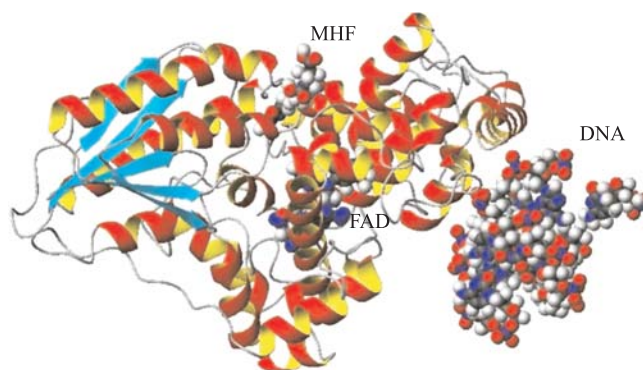


Fig. 2. (Color online). The ribbon structure of a DNA photolyase protein with two cofactors,  $FADH^-$  and MTHF and the DNA chain. The cofactors FAD and MTHF (centres) and DNA (right) are shown as spherical balls

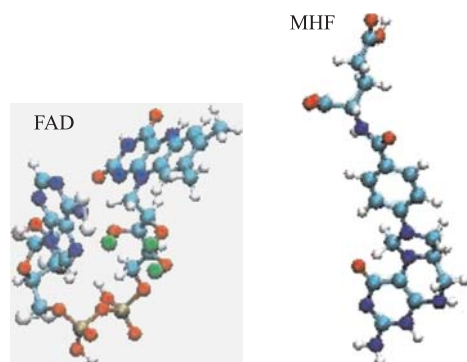


Fig. 3. (Color online). Two cofactors of a DNA photolyase protein,  $\text{FADH}^-$  (left — FAD) and MTHF (right — MHF)

or 8-HDF, acts as a photoantenna and transfers excitation energy to the catalytic  $\text{FADH}^-$  cofactor through nonradiative Forster resonance energy transfer (FRET) — via a dipole — dipole coupling between folate and flavin [2–13].

The conformational behavior of the FAD molecule is very important for understanding the functional and structural properties of the DNA repair protein photolyase. Knowing the FAD, actual conformation can provide insight into the light-driven DNA repair by the DNA photolyase enzyme. The FAD is an essential cofactor for both specific binding to damaged DNA and catalysis. The second chromophore (MTHF or 8-HDF) is not necessary for catalysis and has no effect on specific enzyme — substrate binding.

The conformational peculiarities of the photoactive cofactor FAD were the subject of special interest and were investigated in several studies [10–17]. The X-ray structure analysis of DNA photolyase reveals the U-shaped conformation of the FAD molecule [4]. Based on the molecular dynamics (MD) method, the FAD structure conformation was studied in the gas phase and water in [10–14]. It was found that the FAD molecule could have both «open» I-shaped and «closed» U-shaped conformations. The FAD conformation behavior correlates with DNA photolyase mobility, which is a problem of modern research. In paper [4], using crystal structure coordinates of the substrate-free enzyme from *Escherichia coli*, docking a thymine dimer to the photolyase catalytic site was studied. The molecular dynamics of the system was estimated, and the electron-transfer matrix element between the lowest unoccupied molecular orbitals of flavin and the dimer was calculated. The crystal structure of a DNA photolyase, reported in [5], was found to bind to duplex DNA, which is bent by  $50^\circ$  and forms a synthetic CPD lesion. This CPD lesion is flipped into the active site and split thereby into two thymines by synchrotron radiation at 100 K. In [6], two photolyase-related proteins — PhrA and PhrB — were found to exist in the phytopathogen *Agrobacterium tumefaciens*. It was shown experimentally [7] that photoreactivation prevents UV mutagenesis in a broad range of species. Studies of the Cry-DASH proteins from bacteria, plants, and animals [8] show that they are all actually photolyases with a high degree of specificity for cyclobutane pyrimidine dimers in ssDNA. Despite being tightly wrapped in apo-GOx by nonbonded interaction forces, including vdW forces, and the electrostatic interaction [9], the FAD molecule still exhibits great mobility in the apo-GOx tunnel. A number of structural parameters, including distances, angles, and dihedrals, were introduced in this study to describe the fine structure features and evaluate the mobility of FAD. In [11], the extended FAD molecule also shows a mobility gradient between the very rigid flavin (the mean value of  $\langle B \rangle = 8.7 \text{ \AA}^2$ ) and the more mobile adenine (the mean value of  $\langle B \rangle = 16.2 \text{ \AA}^2$ ). The entire active center is particularly well ordered, with temperature factors around  $10 \text{ \AA}^2$ .

In the present work, the FAD conformational and dynamic behaviors were studied in the whole DNA photolyase enzyme structure. Unlike the earlier works mentioned above, our study simulates the complex structure of the DNA photolyase protein, containing  $\text{FADH}^-$ ,

MTHF, and DNA molecules, and embedded in different water solvent baths. Based on the molecular dynamics (MD) simulation, we aimed to compare the conformational changes of the FAD cofactor with the constituent fragments of the molecular system under consideration.

## 1. MATERIALS AND METHODS

All simulations were performed with the AMBER (versions 8 to 11) MD software package for studying biomolecules [18,19]. The molecular complex of the DNA photolyase protein (containing  $\text{FADH}^-$  and MTHF) and DNA molecules were solvated with a rectangular water model with the number of water molecules equal to 20113 (Fig. 4). The electrostatic interactions were treated with the Particle Mesh Ewald (PME) algorithm [18–21]. The Cornell et al. all-atom force field was used in the MD simulations [22,23]. To build the AMBER parameter/topology input files for the protein,  $\text{FADH}^-$  (FAD), MTHF (MHF) (Table 1), and DNA molecules, the LEaP basic preparation program was used. The atomic charges were provided by the AM1-BCC charge model of the Antechamber program; the combinations of CHARMM and «general AMBER force field (GAFF)» parameters provide the charges closely to the data from [10]; for creating the missing force field parameters, the Parmchk program was used. All systems were solvated with TIP3P molecules [24] produced in a rectangular (periodic) water bath. The temperature was kept constant by using the Berendsen algorithm [25]. Only bond

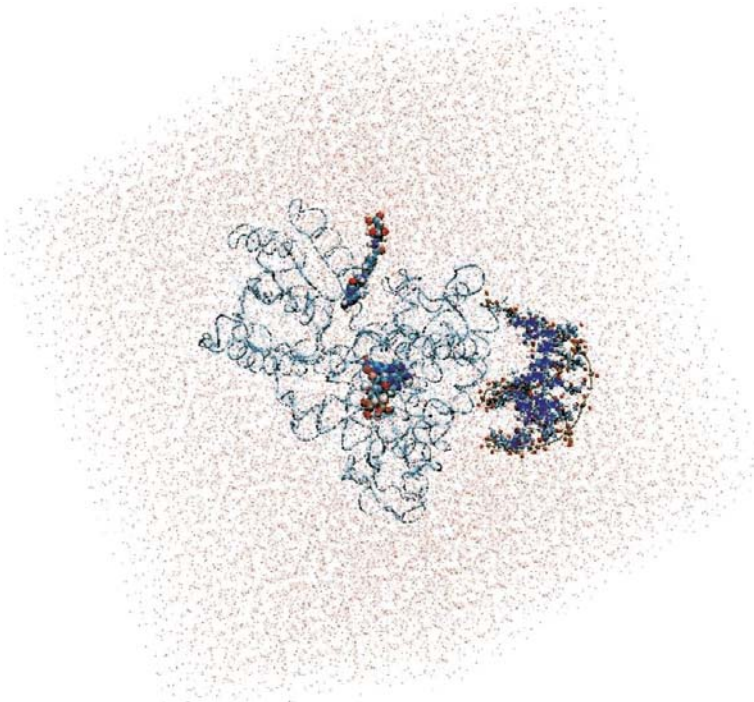


Fig. 4. (Color online). The DNA photolyase protein, containing cofactors  $\text{FADH}^-$  (FAD) and MTHF (MHF) and DNA molecule, solvated by a rectangular (periodic) water bath

Table 1. The masses and charges of FADH<sup>-</sup> (FAD) and MTHF (MHF) molecules with their schematic diagram

Atom	$m/m_e$ , a.m.u.	$q/e$ , pr. charge	Atom	$m/m_e$ , a.m.u.	$q/e$ , pr. charge	Atom	$m/m_e$ , a.m.u.	$q/e$ , pr. charge
O4	16.00	-0.2930	O1P	16.00	-0.8064	NA2	14.01	-0.8848
C4	12.01	+0.4110	HOP2	1.008	+0.5190	HN21	1.008	+0.4008
N3	14.01	-0.5855	O2P	16.00	-0.8083	HN22	1.008	+0.4298
HN3	1.008	+0.3785	O3P	16.00	-0.8278	N1	14.01	-0.7150
C2	12.01	+0.8449	PA	30.97	+1.8425	HN1	1.008	+0.4588
O2	16.00	-0.5015	O1A	16.00	-0.8044	C8A	12.01	+0.2330
N1	14.01	-0.3644	HOA2	1.008	+0.5090	N8	14.01	-0.6990
C10	12.01	+0.1567	O2A	16.00	-0.8393	H8	1.008	+0.3878
C4X	12.01	-0.0843	O5B	16.00	-0.6102	C7	12.01	+0.1508
N5	14.01	+0.0679	C5B	12.01	+0.1664	H71	1.008	+0.0797
HN5	1.008	+0.3597	H51A	1.008	+0.0787	H72	1.008	+0.0677
C5X	12.01	-0.1393	H52A	1.008	+0.0707	C6	12.01	+0.1235
C6	12.01	-0.1000	C4B	12.01	+0.0641	H6	1.008	+0.0777
H6	1.008	+0.1640	H4B	1.008	+0.0887	C9	12.01	+0.1728
C7	12.01	-0.0513	O4B	16.00	-0.4066	H91	1.008	+0.0517
C7M	12.01	-0.0708	C3B	12.01	+0.0921	H92	1.008	+0.0657
HM71	1.008	+0.0727	O3B	16.00	-0.6208	N10	14.01	-0.6400
HM72	1.008	+0.0607	HO3A	1.008	+0.4360	C15	12.01	+0.1836
HM73	1.008	+0.0747	H3B	1.008	+0.1047	C14	12.01	-0.1990
C8	12.01	+0.0537	C2B	12.01	+0.0821	H14	1.008	+0.1390
C8M	12.01	-0.1048	O2B	16.00	-0.5718	C13	12.01	-0.0380
HM81	1.008	+0.0697	HO2B	1.008	+0.4170	H13	1.008	+0.1560
HM82	1.008	+0.1227	H2B	1.008	+0.1217	C16	12.01	-0.1890
HM83	1.008	+0.0747	C1B	12.01	+0.2168	H16	1.008	+0.1530
C9	12.01	-0.1570	H1B	1.008	+0.1407	C17	12.01	-0.0610
H9	1.008	+0.2090	N9A	14.01	-0.2940	H17	1.008	+0.1360
C9A	12.01	+0.1267	C8A	12.01	+0.3877	C12	12.01	-0.1926
N10	14.01	-0.0581	H8A	1.008	+0.0688	C	12.01	+0.6907
C1'	12.01	+0.0113	N7A	14.01	-0.5261	O	16.00	-0.6361
H1'1	1.008	+0.1087	C5A	12.01	-0.2432	N	14.01	-0.5739
H1'2	1.008	+0.1047	C6A	12.01	+0.7672	HN	1.008	+0.3275
C2'	12.01	+0.1091	N6A	14.01	-0.9505	CA	12.01	+0.0217
O2'	16.00	-0.6228	H61A	1.008	+0.4488	CT	12.01	+0.6081
HO2'	1.008	+0.4520	H62A	1.008	+0.4508	O1	16.00	-0.5791
H2'	1.008	+0.0717	N1A	14.01	-0.7850	HO2	1.008	+0.4580
C3'	12.01	+0.1081	C2A	12.01	+0.6999	O2	16.00	-0.4990

End of Table 1

Atom	$m/m_e$ , a.m.u.	$q/e$ , pr. charge	Atom	$m/m_e$ , a.m.u.	$q/e$ , pr. charge	Atom	$m/m_e$ , a.m.u.	$q/e$ , pr. charge
O3'	16.00	-0.6088	H2A	1.008	+0.0611	HA	1.008	+0.0907
HO3'	1.008	+0.4570	N3A	14.01	-0.7370	CB	12.01	-0.0814
H3'	1.008	+0.0867	C4A	12.01	+0.4808	HB1	1.008	+0.0847
C4'	12.01	+0.1021	C11	12.01	+0.4180	HB2	1.008	+0.0667
O4'	16.00	-0.6258	H111	1.008	+0.0847	CG	12.01	-0.1324
HO4'	1.008	+0.4420	H112	1.008	+0.0827	HG1	1.008	+0.0817
H4'	1.008	+0.0577	N5	14.01	-0.5684	HG2	1.008	+0.1077
C5'	12.01	+0.1554	C4A	12.01	-0.0982	CD	12.01	+0.6391
H5'1	1.008	+0.0697	C4	12.01	+0.7257	OE1	16.00	-0.6091
H5'2	1.008	+0.0737	O4	16.00	-0.5621	HOE2	1.008	+0.4460
O5'	16.00	-0.5852	N3	14.01	-0.7301	OE2	16.00	-0.5480
P	30.97	+1.8105	C2	12.01	+0.8331			

lengths involving hydrogen atoms were constrained using the SHAKE method [26]. The results of simulations and images of the simulated proteins were analyzed using the RasMol [27], MOLMOL [28], and Visual Molecular Dynamics (VMD) [29] software.

**1.1. MD Protocol.** We have simulated the behavior of the DNA photolyase enzyme at temperatures  $T = 50$ – $250$  K. An example of the MD protocol for the periodic PME-NVT simulation is presented below:

\*\*\*\*\*

**Potential function:**

ntf = 1, ntb = 1, igb = 0, nsnb = 1, ipol = 0, gbsa = 0, iesp = 0, dielc = 1.0,  
cut = 10.0, intdiel = 1.0, scnb = 2.0, scee = 1.2

**Molecular dynamics:**

nstlim = 10000, nscm = 2, nrespa = 1, t = 0.0, dt = 0.001

**Berendsen temperature regulation:**

temp0 = 200.0, tempi = 0.0, tautp = 0.2

**SHAKE:**

ntc = 2, jfastw = 0, tol = 0.00001

**Ewald parameters:**

verbose = 0, ew\_type = 0, nbflag = 1, use\_pme = 1, Box X = 103.066,  
Box Y = 83.512, Box Z = 96.459, Alpha = 90.0, Beta = 90.0, Gamma = 90.0,  
NFFT1 = 108, NFFT2 = 90, NFFT3 = 100, Cutoff = 10.0, Tol = 0.100E-04,  
Ewald Coefficient = 0.27511

\*\*\*\*\*

## 2. RESULTS AND DISCUSSION

The dynamical changes of a DNA photolyase protein were traced within a long-nanosecond time scale. A photolyase enzyme, two cofactors (FADH<sup>-</sup> and MTHF) fitted into the pocket, and DNA chain located in the vicinity of the enzyme were surrounded by water molecules filling up the entire system as shown in Figs.4 and 5. For the molecular structure under consideration, the positions of several amino acid residues were fixed up and the relative movements of different protein regions were compared to display the interaction between the FADH<sup>-</sup> (FAD), MTHF (MHF), and DNA molecules. The conformational changes of different components in the simulated system were compared through the calculation of the interatomic distances  $d1 - d4(t)$  as shown in Table 2 and Fig.5 (right picture).

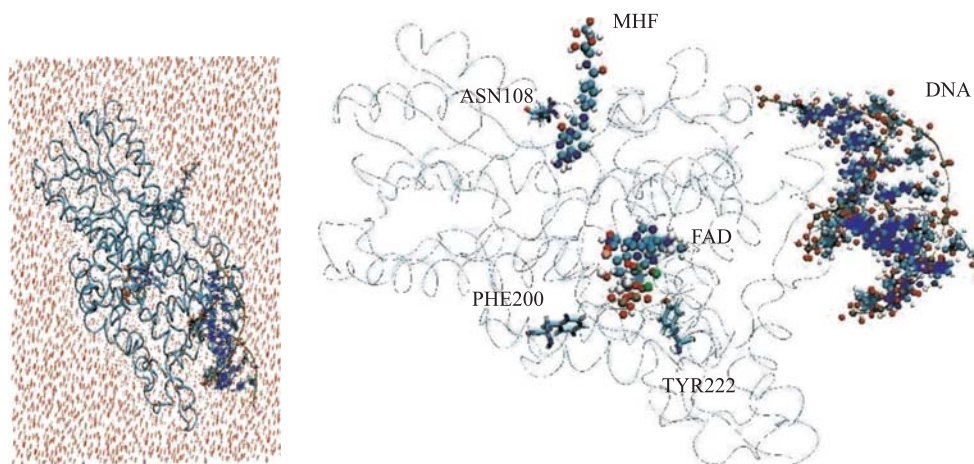


Fig. 5. (Color online). The section of simulated molecular model (left) with the location of molecular components inside the photolyase enzyme (right). The FADH<sup>-</sup> (FAD), MTHF (MHF) cofactor, and DNA chain are shown as spherical balls

Table 2. The initial distances between the DNA photolyase cofactors (MHF, FAD) and neighboring amino acid residues as shown in Fig. 5

Atoms	$d1$ [MHF-ASN108], Å (CD)	$d2$ [FAD-PHE200], Å (C8)	$d3$ [FAD-TYR222], Å (N3A)	$d4$ [DNA-TYR222], Å (P)
N	12.1	30.0	12.3	37.4
CA	11.8	29.7	12.2	38.5
CB	12.0	29.8	10.0	38.2
O	13.0	31.1	12.6	40.1

First, we have estimated the distances between the ASN108 amino acid residue and MTHF molecule. We have estimated the distances between the carbon atom (CD) of the MTHF molecule and other heavy atoms: the nitrogen (N) atom, two carbon (CA, CB), and oxygen (O) atoms of the ASN108 amino acid residue. Figure 6 shows that during a long dynamics simulation, the  $d1$  [MHF-ASN108] distance does not change visibly and it remains

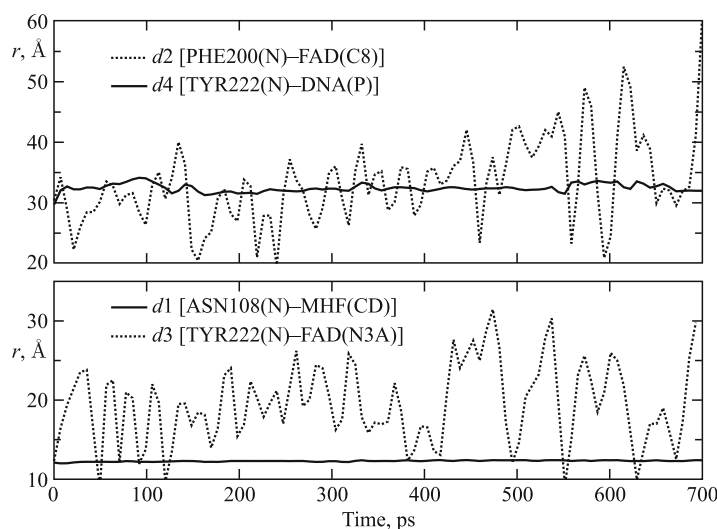


Fig. 6.  $d1-d4(t)$  distance diagrams showing the positional changes in the photolyase protein molecular complex interacting with the DNA chain

as the initial values:  $d1$  [MHF(CD)-ASN108(N, CA, CB, O)]  $\approx 12.0$  Å. All the values of  $d1$  vary negligibly around their initial values, so the MTHF molecule shows a weak relative movement inside the enzyme's pocket during the whole simulation period.

Next, in Fig. 6, the  $d2$  [FAD-PHE200] and  $d3$  [FAD-TYR222] distances for the positional changes of the PHE200 and TYR222 amino acid residues relative to the FADH<sup>-</sup> molecule are shown. The PHE200 and TYR222 residues symmetrically surround the FADH<sup>-</sup> molecule on two sides. For PHE200, we calculated the distances between the carbon atom (C8) of FADH<sup>-</sup> and the nitrogen (N) atom, two carbon (CA, CB), and oxygen (O) atoms. Both distances  $d2$  [FAD-PHE200] and  $d3$  [FAD-TYR222] in Fig. 6 clearly demonstrate the strong oscillating behavior of the FAD molecule. Comparison with the initial distances  $d2$  [FAD(C8)-PHE200(N, CA, CB, O)]  $\approx 30.0$  Å, and  $d3$  [FAD(N3A)-TYR222(N, CA, CB, O)]  $\approx 12.0$  Å, from Fig. 6 is straightforward. In other words, FAD mobility inside the enzyme's pocket looks very high.

Finally, we calculated the positional changes of the DNA chain, which is located in a close contact region with the photolyase protein. Figure 6 also presents a  $d4$  [DNA-TYR222] distance diagram for the TYR222 amino acid residue position relative to the DNA molecule. The initial distance was as follows:  $d4$  [DNA(P)-TYR222(Ni, CA, CB, O)]  $\approx 38.0$  Å. From Fig. 6, it is easy to see that the DNA position relative to the protein segment (viz. TYR222) does not change visibly during a long period of dynamical changes.

The distance diagrams summarized in Fig. 6 compare the  $d1-d4(t)$  dynamics and indicate on differences in the relative positional changes inside the DNA photolyase enzyme. The structural behavior of the DNA photolyase (with FAD and MTHF cofactors) simulated at the temperatures from  $T = 50$  up to  $T = 250$  K shows a high mobility of the FAD molecule inside the enzyme's pocket. At the simulated temperatures, protein parts (MTHF and the DNA chain) as well as water molecules have very low dynamic mobility and show a slow structural movement. At the same time, even starting from low temperatures, the FAD molecule

demonstrates relatively fast dynamics and undergoes rapid structural changes. It is worth noting that in [15] a similar structural behavior of the FAD molecule at low temperatures was observed for another type of a protein complex, namely, for Fre — the NAD(P)H:flavin oxidoreductase. In more detail, the average positions of the nearby TYR35, TYR72, TYR116, and FAD were compared in [15]. Figure 1 [15] shows that the atomic trajectories and center-to-center distances between three TYR residues and the FAD isoalloxazine ring also indicate high FAD mobility at low temperatures.

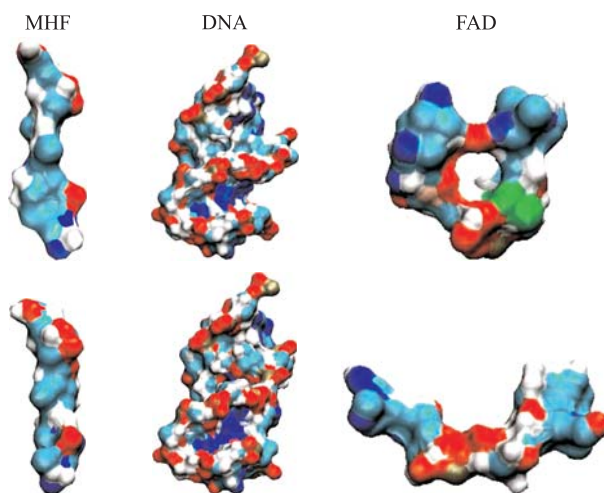


Fig. 7. (Color online). The initial (top) and final (bottom) configurational shapes of the MTHF (left — MTHF), DNA (middle), and FADH<sup>-</sup> (right — FAD) molecules during the DNA photolyase structure relaxation

In Fig. 7, the dynamic molecular surfaces of the MTHF, DNA, and FAD molecules are compared. It is clear that the MTHF and DNA molecules undergo negligible configuration changes; MTHF and DNA remain in a frozen state at a low temperature. At the same time, the FAD configuration changes periodically throughout the simulation period, tending from the «closed» U-shaped to the «open» I-shaped one. Such a FAD configuration behavior looks like «butterfly motion» [10, 15]. It should be stressed that the transition from the U-shaped configuration, the FAD's original one revealed by X-ray structure analysis, to the I-shaped configuration results in the FAD molecule not being allowed to stay more inside the enzyme pocket. Obviously, the DNA photolyase enzyme cannot properly locate FAD's I-shaped configuration and keep FAD at a binding site.

It is worth noting that the unique FAD-binding domain with its high degree of sequence identity in the environment forms a family of highly homologous photolyase/cryptochrome proteins. From bacteria to mammals, these two types of proteins carry out distinct functions: photolyase harnesses blue light energy to break bonds and repair UV photoproducts in DNA; and cryptochrome is a sensor of environmental light-regulating circadian entrainment in animals and plants [12]. The FAD chromophore binding inside the DNA photolyase pocket has many similarities with 11-*cis* retinal chromophore in opsin proteins [30–36]. Opsins are expressed in rods and cones in the back (outer) part of the retina; photolyase/cryptochrome

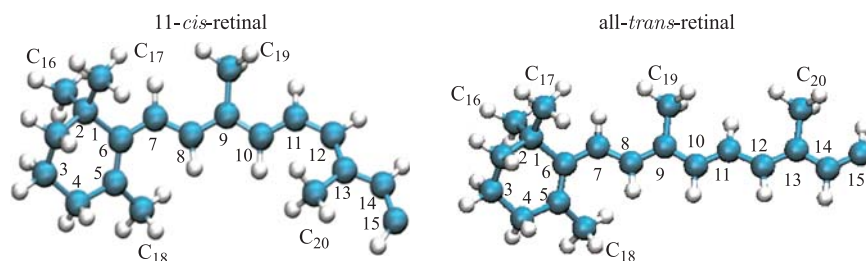


Fig. 8. The retinal chromophore configurations, 11-*cis*-retinal (left) and all-*trans*-retinal (right), in the binding pocket of visual pigment rhodopsin

proteins are expressed in the front (inner) part of the retina. Opsins initiate phototransduction by *cis-trans* isomerization of retinal by light; the transition from 11-*cis* to all-*trans* (Fig. 8) puts 11-*cis* retinal out of the protein binding. Thus, all-*trans*-retinal behaves like I-shaped FAD and cannot be allowed to stay any longer inside the chromophore pocket. On the other hand, the FAD chromophore, as its form changes from the «closed» U-shaped to the «open» I-shaped, should also leave the protein. Thus, two photosensory systems in mammals — the 3D visual system and the circadian photosensory system, are correlated by their chromophores. We should note that for the opsin + retinal photoreceptors, the signal phototransduction mechanism is already known; for the cryptochromes (circadian photoreceptors with the folate (MTHF) and flavin (FAD) chromophores), the phototransduction mechanism is still unknown [2].

## CONCLUSIONS

MD simulations were performed on the DNA photolyase enzyme structure with two chromophore cofactors (FADH<sup>-</sup> and MTHF), which are required for the enzyme functioning. FAD is essential for both specific binding to damaged DNA and catalysis. In a long nanosecond scale, dynamical changes were traced in a molecular system consisting of the photolyase enzyme, FAD and MTHF cofactors fitted into the enzyme's pocket, and a DNA chain located in the vicinity of the enzyme; the system was solvated with different water models. The structural behavior of the DNA photolyase (with FAD and MTHF cofactors) was simulated at low temperatures from  $T = 50$  to 250 K. The distance diagrams for the key fragments of the DNA photolyase were built, and the comparison of the positional dynamics indicates different relative mobility. The FAD molecule has relatively high mobility inside the enzyme's binding pocket. The dynamic molecular surfaces of the MTHF, DNA, and FAD molecules reveal transition of the FAD conformation from a «closed» U-shaped to an «open» I-shaped one. Such a behavior of FAD inside the DNA photolyase enzyme can be an important factor for this enzyme binding to UV-damaged DNA and the following DNA repair mechanism. Similarities were discussed between the two photosensory systems: the visual pigment rhodopsin providing 3D vision and the photolyase/cryptochrome proteins responsible for the circadian function. Their structure correlations were found to be based on the similarities between the FAD chromophore binding inside the DNA photolyase pocket and 11-*cis* retinal binding inside the opsin's chromophore centre

**Acknowledgements.** The work has been performed within a research collaboration between JINR (Russia) and Keio University (Japan) and was supported by the JSPS (Japan Society for the Promotion of Science)–RFBR (Russian Foundation for Basic Research) (grant No.13-04-92100). The work has been supported in part by the Grant in Aid for the Global Centre of Excellence Program to the Centre for Education and Research of Symbiotic, Safe and Secure System Design from Japan’s Ministry of Education, Culture, Sport, and Technology. The MD simulations have been performed using computing facilities, software, and clusters at JINR, Russia (CICC), RIKEN, Japan (RICC), and the Yasuoka Laboratory at Keio University, Japan. We thank Prof. Vladimir Korenkov (LIT, JINR) for providing us with computer time at CICC. The authors would like to specially thank Mr. Sergei Negovetov (JINR) for technical assistance and helpful comments.

## REFERENCES

1. *Gleiser M.* From Cosmos to Intelligent Life: The Four Ages of Astrobiology. <http://arxiv.org/abs/1202.5042>.
2. *Sancar A.* Structure and Function of DNA Photolyase and Cryptochrome Blue-Light Photoreceptors // *Chem. Rev.* 2003. V. 103. P. 2203–2237.
3. *Tamada T. et al.* Crystal Structure of DNA Photolyase from *Anacystis Nidulans* // *Nat. Struct. Biol.* 1997. V. 4(11). P. 887–891; doi: 10.1038/nsb1197-887.
4. *Antony J., Medvedev D., Stuchebrukhov A.* Theoretical Study of Electron Transfer between the Photolyase Catalytic Cofactor FADH<sup>−</sup> and DNA Thymine Dimer // *J. Am. Chem. Soc.* 2000. V. 122. P. 1057–1065.
5. *Mees A. et al.* Crystal Structure of a Photolyase Bound to a CPD-Like DNA Lesion after in situ Repair // *Science.* 2004. V. 306. P. 1724; doi: 10.1126/science.1101598.
6. *Oberpichler I. et al.* A Photolyase-Like Protein from *Agrobacterium Tumefaciens* with an Iron-Sulfur Cluster // *PLoS ONE.* 2011. V. 6(10). P. e26775; doi: 10.1371/journal.pone.0026775.
7. *Lucas-Lledó J.I., Lynch M.* Evolution of Mutation Rates: Phylogenomic Analysis of the Photolyase/Cryptochrome Family // *Mol. Biol. Evol.* 2009. V. 26(5). P. 1143–1153; doi: 10.1093/molbev/msp029.
8. *Selby C.P., Sancar A.* A Cryptochrome/Photolyase Class of Enzymes with Single-Stranded DNA-Specific Photolyase Activity // *PNAS.* 2006. V. 103(47). P. 17696–17700; doi: 10.1073/pnas.0607993103.
9. *Liu F. et al.* Conformational Mobility of GOx Coenzyme Complex on Single-Wall Carbon Nanotubes // *Sensors.* 2008. V. 8. P. 8453–8462; doi: 10.3390/s8128453.
10. *Hahn J., Michel-Beyerle M.-E., Rösch N.* Conformation of the Flavin Adenine Dinucleotide Cofactor FAD in DNA-Photolyase: A Molecular Dynamics Study // *J. Mol. Model.* 1998. V. 4. P. 73–82; doi: 10.1007/s008940050133.
11. *Karplus P.A., Schulz G.E.* Refined Structure of Glutathione Reductase at 1.54 Å Resolution // *J. Mol. Biology.* 1987. V. 195(3). P. 701–729; [http://dx.doi.org/10.1016/0022-2836\(87\)90191-4](http://dx.doi.org/10.1016/0022-2836(87)90191-4).
12. *Thompson C.L., Sancar A.* Photolyase/Cryptochrome Blue-Light Photoreceptors Use Photon Energy to Repair DNA and Reset the Circadian Clock // *Oncogene.* 2002. V. 21. P. 9043–9056.
13. *Verma P.K., Pal S.K.* Ultrafast Resonance Energy Transfer in Biomolecular Systems // *Eur. Phys. J. D.* 2010. V. 60. P. 137–156.
14. *Park H.-W. et al.* // *Science.* 1995. V. 268. P. 1866.

15. Guobin Luo *et al.* Dynamic Distance Disorder in Proteins Is Caused by Trapping // *J. Phys. Chem. B.* 2006. V. 110(19). P. 9363–9367.
16. Wang Y., Gasper P. P., Taylor J. S. // *J. Am. Chem. Soc.* 2000. V. 122. P. 5510.
17. Masson F. *et al.* A QMMM Investigation of Thymine Dimer Radical Anion Splitting Catalyzed by DNA Photolyase // *ChemPhysChem.* 2009. V. 10. P. 400–410.
18. Pearlman D. A. *et al.* AMBER, a Computer Program for Applying Molecular Mechanics, Normal Mode Analysis, Molecular Dynamics and Free Energy Calculations to Elucidate the Structures and Energies of Molecules // *Comp. Phys. Commun.* 1995. V. 91. P. 1–41.
19. Case D. C. *et al.* // AMBER. 2010.
20. Essmann U. *et al.* // *J. Chem. Phys.* 1995. V. 103. P. 8577–8592.
21. Kholmurodov K. *et al.* A Smooth-Particle Mesh Ewald Method for DL\_POLY Molecular Dynamics Simulation Package on the Fujitsu VPP700 // *J. Comp. Chem.* 2000. V. 21(13). P. 1187–1191.
22. Ponder J. W., Case D. A. Force Fields for Protein Simulations // *Adv. Prot. Chem.* 2003. V. 66. P. 27–85.
23. Cornell W. D. *et al.* A Second Generation Forth Field for the Simulation of Proteins and Nucleic Acids // *J. Am. Chem. Soc.* 1995. V. 117. P. 5179–5197.
24. Jorgensen W. L., Chandrasekhar J., Madura J. D. Comparison of Simple Potential Functions for Simulating Liquid Water // *J. Chem. Phys.* 1983. V. 79. P. 926–935.
25. Berendsen H. J. C. *et al.* Molecular Dynamics with Coupling to an External Bath // *J. Chem. Phys.* 1984. V. 81. P. 3684–3690.
26. Ryckaert J. P., Ciccotti G., Berendsen H. J. C. Numerical Integration of the Cartesian Equations of Proteins and Nucleic Acids // *J. Comp. Phys.* 1997. V. 23. P. 327–341.
27. Sayle R. A., Milner-White E. J. RasMol: Biomolecular Graphics for All // *Trends in Biochem. Sci.* 1995. V. 20. P. 374–376.
28. Koradi R., Billeter M., Wuthrich K. MOLMOL: a Program for Display and Analysis of Macromolecular Structure // *J. Mol. Graphics.* 1996. V. 4. P. 51–55.
29. Humphrey W., Dalke A., Schulten K. VMD — Visual Molecular Dynamics // *Ibid.* P. 33–38.
30. Mirzadegan T. *et al.* Sequence Analyses of G-Protein-Coupled Receptors: Similarities to Rhodopsin // *Biochemistry.* 2003. V. 42. P. 2759–2767.
31. Gether U., Kobilka B. K. G Protein-Coupled Receptor // *J. Biol. Chem.* 1998. V. 273. P. 17979–17982.
32. Palczewski K. *et al.* Crystal Structure of Rhodopsin: a G-Protein-Coupled Receptor // *Science.* 2000. V. 289. P. 739–745.
33. Okada T. *et al.* The Retinal Conformation and Its Environment in Rhodopsin in Light of a New 2.2 Å Crystal Structure // *J. Mol. Biol.* 2004. V. 342. P. 571–583.
34. Salgado G. F. J. *et al.* Deuterium NMR Structure of Retinal in the Ground State of Rhodopsin // *Biochemistry.* 2004. V. 43. P. 12819–12828.
35. Teller D. C. *et al.* Advances in Determination of a High-Resolution Three-Dimensional Structure of Rhodopsin, a Model of a G-Protein-Coupled Receptor (GPCRs) // *Biochemistry.* 2001. V. 40. P. 7761–7772.
36. Kholmurodov Kh. T., Feldman T. B., Ostrovskii M. A. Molecular Dynamics of Rhodopsin and Free Opsin: Computer Simulation // *Neuroscience and Behavioral Physiology.* 2007. V. 37(2). P. 161–174.

Received on February 13, 2013.